Carbon 223 (2024) 118946

Contents lists available at ScienceDirect

Carbon

journal homepage: www.elsevier.com/locate/carbon

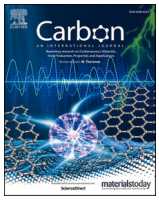

Inductively coupled plasma spectroscopy for heteroatom-doped carbonaceous materials: Limitations and acid choice for digestion

Rémi F. André [a,*], Jessica Brandt [a], Johannes Schmidt [b], Nieves López-Salas [a,c], Mateusz Odziomek [a], Markus Antonietti [a]

[a] Colloid Chemistry Department, Max Planck Institute of Colloids and Interfaces, 14476, Potsdam, Germany
[b] Department of Chemistry, Functional Materials Technische Universität Berlin, 10623, Berlin, Germany
[c] Chair of Sustainable Materials Chemistry, Paderborn University, Warburger Strass 100, 33098, Paderborn, Germany

ARTICLE INFO

Keywords:
Digestion method
Elemental analysis
Heteroatom doping
ICP
P-doped carbon

ABSTRACT

Heteroatom-doped carbonaceous materials have garnered significant attention in the fields of catalysis, energy conversion and storage, and pollutant recovery. However, accurately determining the doping extent remains a delicate task in a number of cases (*e.g.* phosphorus, boron, selenium), often leading to conflicting data from different characterization techniques. Inductively Coupled Plasma (ICP) spectroscopy stands out as a routine technique; nevertheless, reliable results necessitate appropriate digestion protocols. In this study, we demonstrate on a series of P-doped samples, with P contents ranging from 2 to 14 *wt%*, how the choice of acids (HCl, HNO_3, H_2SO_4) and oxidizing compounds (H_2O_2) for digestion drastically affects the results, with variations of up to 620 %. Though commonly used, *aqua regia* proved highly unreliable, particularly for P-doped carbon nitrides, while piranha solution appeared as a promising alternative, with a precision, *i.e.* a coefficient of variation, *ca.* 5.0 %. The contents deriving from piranha solution digestion were subsequently comforted through X-ray Photoelectron Spectroscopy. We finally put in perspective the use of ICP in terms of sensitivity and accuracy with the main analytical techniques employed in literature to determine the element composition of carbon materials.

1. Introduction

The introduction of heteroatoms into carbon materials represents a widely employed strategy to fine-tune the electronic properties of carbon nanostructures, and thereby affecting their stability, energy storage capabilities, or catalytic activity [1–6]. Nitrogen, oxygen, and sulfur are the most frequently encountered dopants; however, recent years have seen significant research on phosphorus-doped carbonaceous materials and carbon nitrides, particularly for their applications in thermal catalysis [7], electrocatalysis [8], and photocatalysis [9]. Their rich chemistry arises from the diverse potential environments that phosphorus atoms can occupy, extending beyond the usual phosphoric acid group. X–ray Photoelectron Spectroscopy (XPS) and Nuclear Magnetic Resonance (NMR) represent the prevailing techniques for discerning the speciation among various chemical species, a crucial aspect for rationalizing catalysis mechanisms or material performance.

The assessment of the total content holds equally significant importance, especially for estimating the density of active sites in catalysts or to engage into theoretical modeling. However, the accuracy of such measurements is sometimes neglected or overlooked, and the associated error margins are seldom reported. In the case of carbonaceous materials, Scanning Electron Microscopy coupled with Energy-Dispersive X-ray Spectroscopy (SEM-EDX) and XPS can provide quantitative data, but they exhibit limitations in accuracy when dealing with light elements. Additionally, sample morphology and heterogeneities may introduce significant biases in the results [10–12]. Unlike nitrogen (N), oxygen (O), and sulfur (S), where Elemental Combustion Analysis (ECA), commonly known as "CHNS analysis", offers more reliable measurements with minimal material mass, direct analysis by combustion is not possible for materials doped with phosphorus (P), but also boron (B) and selenium (Se) [3,13,14]. Consequently, Inductively Coupled Plasma (ICP) spectroscopy is the technique of choice due to its limited bias and high sensitivity [15,16]. Contrary to all the previously mentioned techniques, it nonetheless requires the digestion of the material prior to analysis.

The majority of wet digestion methods involves combinations of

* Corresponding author.
E-mail address: remi.andre@mpikg.mpg.de (R.F. André).

https://doi.org/10.1016/j.carbon.2024.118946
Received 21 November 2023; Received in revised form 27 January 2024; Accepted 16 February 2024
Available online 27 February 2024

acids (*e.g.* HNO_3, $HClO_4$, H_2SO_4, HCl, HF) and, in certain instances, hydrogen peroxide (H_2O_2) [17–24]. Recently, Gunatilake et al. conducted a comparative study on biochars for metal content quantification, evaluating the efficiency of an open vessel digestion, chosen for its convenience, and a microwave-assisted digestion, which allows for higher temperatures under pressure [19]. The open vessel digestion protocol was successful solely for low-temperature pyrolyzed carbons when using an H_2SO_4/H_2O_2 mixture. By employing fuming nitric acid at 180 °C in an autoclave, it was nonetheless possible to enhance the extent of digestion for the other materials. Costa et al. also attested of the high chemical recalcitrance of sp^2-rich carbons (carbon nanotubes, graphite, graphene) and could not reach total decomposition even when utilizing a two-step protocol with a HNO_3/H_2O_2 mixture at 220 °C [18]. Additionally, various studies have specifically focused on quantifying metal traces in carbon nanotubes and have developed methods based on alkaline oxide melt combustion [25], Microwave-Induced Combustion (MIC) by oxygen [24], or microwave-assisted oxidation [23,26]. While achieving complete digestion of carbon black, biochars, and graphenic carbon materials presents considerable challenges due to the immense stability of elemental carbon in aqueous solutions, and concentrated the research efforts so far [27], to the best of our knowledge, no comparable study has been conducted on heteroatom-doped carbonaceous materials thus far.

Despite the importance of the parameters of the digestion step, the preparation step of the sample in analytical chemistry is rarely detailed, and the field of carbon materials is no exception to that rule. As an illustration, out of a selection of 55 articles mentioning the use of ICP for elemental composition of carbonaceous materials (29 for B- or P-doped carbonaceous materials, 4 for checking the absence of metals, and 22 for carbon supported metal-containing nanoparticles), only 12 gave details of the pre-treatment of the material prior to ICP analysis (see the full list in SI). Of these, 4 mentioned microwave-assisted acidic digestion, 4 open vessel digestion in concentrated acids, and 4 mineralization of the sample in a muffle furnace. These statistics by no means indicate a percentage of erroneous results but rather illustrate the frequent lack of information given to the readers about digestion protocols when the focus is put on the materials performance, unless specific equipment or procedures are used. Overall, there is still a likely underestimation of the extent of doping in some of these works.

The primary aim of this study is to assess the significance of the digestion protocol for subsequent ICP analysis of heteroatom-doped carbons (*e.g.* P, B, Se). The comparison is made between digestion using *aqua regia* (HCl/HNO_3 mixture) and *piranha solution* (H_2SO_4/H_2O_2 mixture). To achieve this, the digestibility of different carbonaceous materials (carbon black, N-and P-doped samples, carbon nitride) was first qualitatively evaluated. Then, a series of P-doped materials, designed to represent diverse material structures, were synthesized. We thoroughly analyzed the reproducibility of measurements and identified various sources of errors, along with the underlying chemical processes during digestion. As the ICP is the method of choice for determination of metals deposited on carbon, we also verified the suitability of the different etching for the digestion of a potential metallic part through the study of Ni-containing samples. Finally, an overall comparison of the common techniques for element content determination in nanomaterials is provided in the discussion.

2. Experimental section

Caution: all acidic solutions should be prepared, used and disposed of with care [28]. The materials syntheses are detailed in the Supporting Information.

2.1. Digestion protocols and ICP

The samples were dried under vacuum at 150 °C overnight and a small portion of 10–30 mg was precisely weighed in a 10 mL glass volumetric flask. *Aqua regia (AR) protocol*: 2 mL of HCl 37 % and 1 mL of HNO_3 65 % were added to *in situ* form *aqua regia* (red-brown solution with characteristic pungent smell). The mixture was let to react 16 h at r. t. and 1 h at 90 °C before being diluted to 10 mL with Milli-Q water. *Piranha solution (PS) protocol:* 3 mL of H_2SO_4 95 % and 1 mL of H_2O_2 50 % were *slowly* added to *in situ* form the *piranha solution* (colorless solution with high effervescence). The mixture was heated up to 90 °C and an extra 1 mL of H_2O_2 50 % was carefully added while hot after 30 min, and another one after 6 h. The solution was left to react for further 16 h, then let to cool down and finally carefully neutralized with Milli-Q water up to 10 mL. If the sample dissolves, the aspect of the solution evolves in the first minutes, but visual differences may be observed up to 16 h (typically lightning of the yellow/brown color). *ICP:* the digestion crudes were diluted 10 times before the Inductively Coupled Plasma Optical Emission Spectroscopy (ICP-OES) measurement was performed with a PerkinElmer ICP-OES Optima 8000. Standard operating conditions were used (Plasma power 1300 W, plasma flux 12 L min^{-1}, nebulizer gas flux 0.55 L min^{-1}, auxiliary gas flux 0.2 L min^{-1}, sample uptake 1.7 mL min^{-1}, Ar purging of the optical part of the instrument). P and Ni were quantified using respectively the 213.6 and 231.6 nm lines using an axial plasma view. The instrument was calibrated using standard solutions from Carl Roth with at least three calibration points (0.5, 5 and 50 ppm): $NH_4H_2PO_4$ solution for phosphorus and Multi-Element ICP Standard Solution IV for nickel. The measurements were performed in triplicate.

2.2. Materials characterization

XPS measurements were performed using a Thermo Fisher Scientific K-Alpha, and data were treated with CasaXPS software. Monochromatic X–ray radiation of 1486.6 eV (Al Kα) was used to analyze each material. The powders were pressed on a carbon tape deposited on the sample holder in order to have a homogeneous layer. Survey scans were obtained using a pass energy of 200 eV and step size of 1 eV, with a spot size of approximately 100 μm. High resolution spectra of C 1s (280–298 eV), N 1s (394–404 eV), O 1s (526–545 eV) and P 2p (125–144 eV) were recorded using a pass energy of 50 eV and step size of 0.1 eV. The binding energy was calibrated against the 284.8 eV peak of adventitious carbon (C–C) [29]. Relative Sensitivity Factors (RSF) of 1, 1.8, 2.93 and 1.19 were used for C, N, O and P, respectively. Unless otherwise stated, a Shirley-type background was used and peaks were deconvoluted using mixed Gauss-Lorentz sum function line shape GL(30). Powder X-ray Diffraction (PXRD) measurements were performed on a Rigaku SmartLab diffractometer, using Cu Kα radiation at 1.5406 Å, with steps of 0.1° and a scanning rate of 0.5° min^{-1}. Physisorption measurements were performed on a Quantachrome Quadrasorb SI apparatus with N_2 adsorption at 77 K after degassing at 150 °C during 15 h. The specific surface area (S_{BET}) of each material was obtained from the N_2 adsorption data ($P/P_0 < 0.2$) using the Brunauer–Emmett–Teller (BET) method. SEM was performed on a LEO 1550 Gemini Zeiss microscope at 5 keV beam energy after sputtering of 5 nm of carbon on top of the samples. EDX was performed using an Oxford Instruments EDX analyzer.

3. Results and discussion

3.1. Aqua regia vs. piranha solution

The efficiency of the digestion step of heteroatom-doped carbonaceous materials with *aqua regia* (AR) or *piranha solution* (PS) was first qualitatively evaluated on a commercial carbon black, a commercial carbon nitride (C_3N_4), a P-doped sample from phytic acid calcination (PA-carbon) and an N-doped one from cytosine calcination (see SI for details on syntheses). Digestion protocols consisted in the use of *aqua regia* (HCl 37 % + HNO_3 65 %) for 16 h at room temperature followed by 1 h at 90 °C (AR protocol), or with *piranha solution* (H_2SO_4 95 % + H_2O_2 50 %) at room temperature followed by 16 h at 90 °C (PS protocol). In

the latter case, hydrogen peroxide was carefully added in three 1 mL portions. A single portion of 1 mL did trigger an effect but bubbling stopped for most samples after only a few minutes, suggesting total consumption of H_2O_2. Note that most of the visual changes occur within the first hour with PS and that the 16 h duration was likely not required. A lower reaction duration at 90 °C was used with *aqua regia* as the reactive gases quickly escaped from the solution at this temperature. The characteristic red color due to nitrogen dioxide indeed vanished within the first hour at 90 °C. All sample digestions appeared similar in the case of the AR protocol: formation of a typical reddish color after a few minutes without any further drastic change in the appearance of the suspension (Fig. 1A). In the case of the PS protocol, a typical effervescence took place: moderate for carbon black, weak at the beginning and then violent for carbon nitride (associated with high heat production), and intense for PA-carbon and N-doped carbon. In the PA-carbon and N-doped carbon cases, the solution rapidly turned brown due to dissolved species, and the color lightened with time, while almost no solid material present in the end (Fig. 1B). A total transparency was obtained for the carbon nitride solution, whose cloudiness gradually decreased to yield a clear solution. The more intense effervescence and higher heat release in the case of carbon nitride with PS is likely due to a faster material decomposition kinetics. Optical transparency is not strictly synonymous with the total digestion of a material, but the decomposition appeared here quasi-total with PS for all samples except carbon black, whereas none was correctly digested by AR.

3.2. Quantitative assessment on P-doped carbons

A series of P-doped carbonaceous materials were synthesized in an attempt to represent a panel of structures and synthetic strategies, *i.e.*, bottom up *vs.* post-treatment (Table 1). In brief, the two P-doped samples were prepared by heat treatment of commercial carbon black (CB) in the presence of H_3PO_4 (P-CB sample (**1**)) [30], and by carbonization of phytic acid (PA-carbon sample (**2**)) [7]. The two P-doped carbon nitrides were obtained by heat treatment of a mixture of dicyandiamide (DCDA) and H_3PO_4 (P–CN-mix sample (**3**)) [9], and by thermal post-treatment of commercial C_3N_4 in the presence of H_3PO_4 (P–CN-post sample (**4**)). Powder X–Ray Diffraction (PXRD) measurements confirmed the turbostratic structure of materials **1** and **2** with the presence of typical broad peaks at 26° and 43°, and the carbon nitride (CN) one for **3** and **4** with the characteristic peaks at 13° and 28° (Fig. 2A). In addition of PXRD, samples **3** and **4** display a pale-yellow color, typical of CN. Nitrogen physisorption experiments at 77 K revealed the much porous nature of **1** and **2** ($S_{BET} > 1000$ m^2 g^{-1}), compared to **3** and **4** ($S_{BET} < 15$ m^2 g^{-1}) (Fig. 2B). According to SEM, all samples are composed of chunks without definite structures at the micron scale. The morphology of **1** and **2,** composed of aggregated colloids <100 nm, appeared rougher than that of **3** and **4**, displaying smoother surfaces, in agreement with the higher porosities of the first ones (Fig. 2C).

Along with ICP, XPS is the most employed technique to access elemental composition of materials. The model materials were therefore characterized following a procedure as representative as possible as to the usual sample preparation and data curation (see Experimental section). Only carbon, nitrogen (for **3**–**4**), oxygen and phosphorus significantly contribute to the surface chemistry (**Table S1** for element compositions). Phosphorus contents of 2.1, 6.4, 14.6 and 8.8 *wt*% were recorded for samples **1** to **4**, respectively. The oxygen to phosphorus ratio O/P, comprised between 2.6 and 5.0, is coherent with pendant phosphate groups (PO_4), while the carbon to nitrogen ratio C/N, of 1.5 and 0.9 for **3** and **4**, consists in an extra evidence of the carbon nitride structure (C_3N_4). One may note the C/N ratio is higher when numerous phosphorus-containing groups are present, likely because the latter replace part of nitrogen-functional groups. The deconvolutions of the

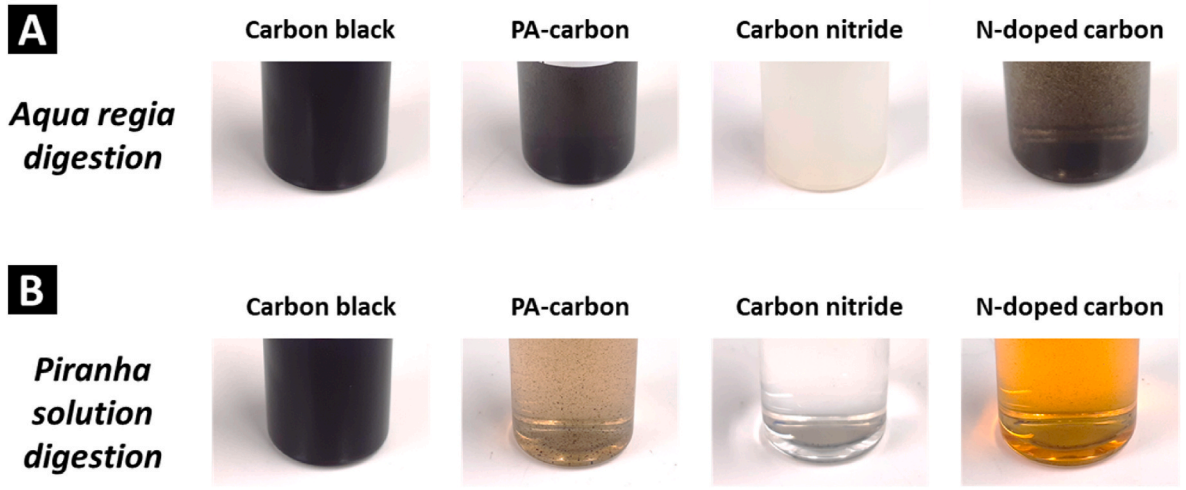

Fig. 1. Qualitative assessment of the efficiency of the digestion. Photographs of the digestion crudes of different carbonaceous materials after (A) treatment in *aqua regia* for 16 h at r.t. and 1 h at 90 °C, (B) treatment in *piranha solution* for 16 h at 90 °C. (A colour version of this figure can be viewed online.)

Table 1
P-doped and Ni-containing carbonaceous materials studied in this work with the corresponding precursors and specific surface areas.

N°		Precursors	Synthetic strategy	S_{BET} (m^2 g^{-1})
1	P-CB	Carbon black, H_3PO_4	Post-treatment	1175
2	PA-carbon	Phytic acid	Bottom-up	1323
3	P–CN-mix	Dicyandiamide, H_3PO_4	Bottom-up	4
4	P–CN-post	C_3N_4, H_3PO_4	Post-treatment	13
5	Ni-CB	Carbon black, $NiCl_2$	Post-treatment	1220
6	Ni–C_3N_4	C_3N_4, $NiCl_2$	Post-treatment	7
7	Ni–N-doped-carbon	Cytosine, $NiCl_2$	Post-treatment	691

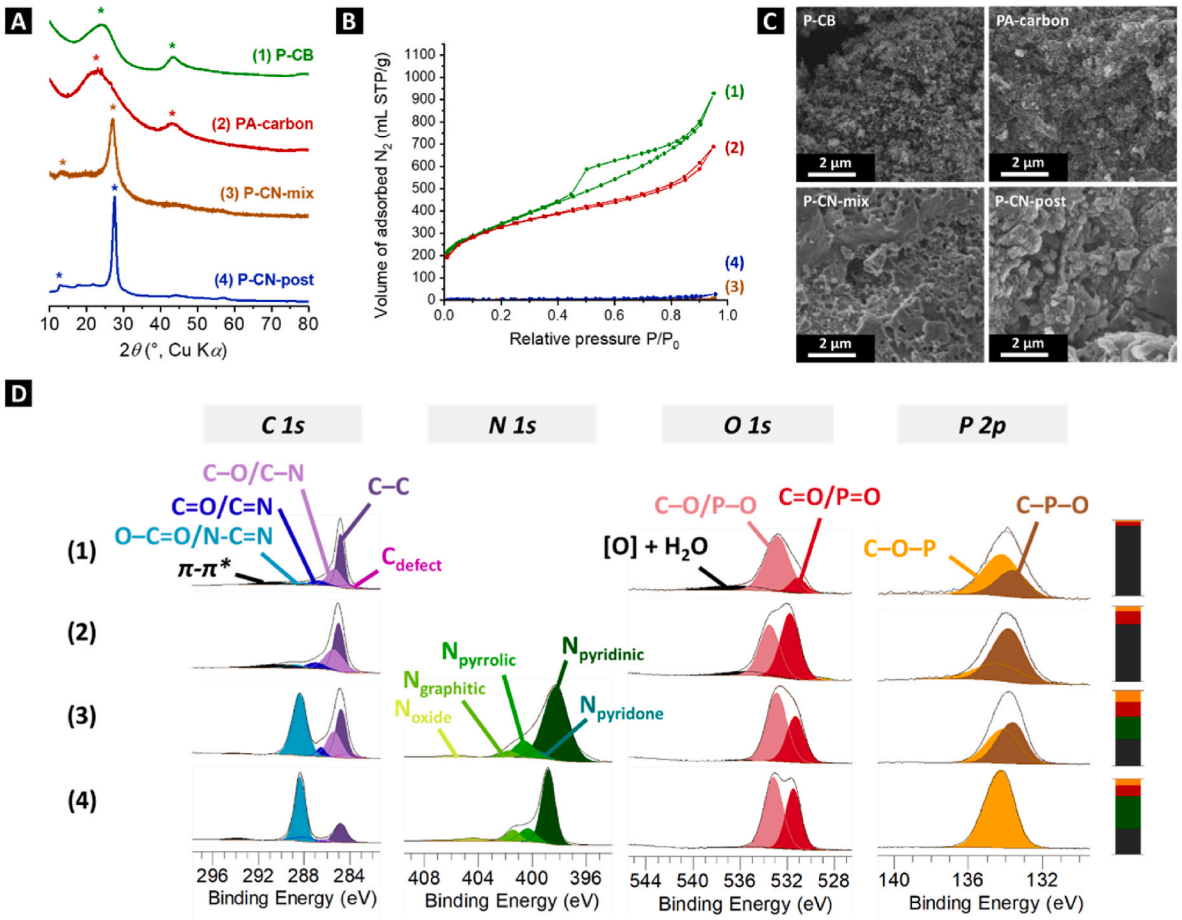

Fig. 2. (A) Powder X–Ray Diffraction patterns of P-doped samples with characteristic peaks of turbostratic carbon and carbon nitride C_3N_4. (B) Nitrogen sorption experiments on samples **1**–**4**. (C) SEM images of samples **1**–**4**. (D) C 1s, N 1s, O 1s and P 2p (from left to right) XPS spectra and deconvolution of samples **1**–**4** (from top to bottom). Details as to peak attribution are given in SI. The C–P–O and C–O–P contributions in P 2p region may also include C–P–N and C–N–P ones. Bars at the right correspond to the element composition in *wt*% (black = carbon, blue = nitrogen, red = oxygen, orange = phosphorus). (A colour version of this figure can be viewed online.)

different regions were performed according to previous works (**Tables S2–4**) [4,29–32]. The presence of reduced phosphorus P(0)/R_3P (130.2 eV) and of phosphorus pentoxide P_4O_{10} (136.0 eV) could be excluded in all cases but at least two components were required for a proper fit of the region (Fig. 2D). The exact attribution of the components is still debated in literature but one may find the distinction between *electron-rich* phosphorus, denoted C–P–O and accounting for structures with at least one C–P bond such as $R_3P{=}O$ (132.5 eV) or phosphonic acids (133.2 eV), and *electron-poor* phosphorus, denoted C–O–P and accounting for phosphate like structures (134.0 eV) with only P–O bonds [4,30,32]. Finally, the important contribution of N–C=N component in the C 1s region of the carbon nitrides agrees with their conjugated structure. The proportion of this component is noticeably higher for P–CN-post which presents the lower C/N ratio (0.9 *versus* 0.75 for C_3N_4), revealing again that the ideal C_3N_4 structure is less affected due to phosphorus insertion if compared with P–CN-mix.

All P-doped materials were subjected to four independent digestions with both AR and PS protocols. Afterward, ICP measurements of the diluted crudes, performed in triplicate, allowed a quantitative assessment of the digestion protocols. The results are summarized in Table 2 and represented graphically in Fig. 3. One can estimate the precision, *i.e.*, the reproducibility, of the protocol, through the coefficient of variation (CV) of the measurement, *i.e.*, the standard deviation normalized by the mean. The lower the CV is, the more reproducible the protocol is. The CV of the whole digestion protocol ($CV_{digestion+ICP}$) was of *ca.* 5 % for both AR and PS, while a typical CV of ICP measurements alone

Table 2
Evaluation of the precisions of the ICP method for determining phosphorus content in carbonaceous materials (in *wt*%) with *aqua regia* or *piranha solution*. Standard deviations (SD) and coefficients of variation (CV) are determined based on 4 independent digestions (reported values correspond to the faded points in Fig. 4).

	ICP – phosphorus (CV: 1.2 %)				
	Aqua regia		Piranha solution		Ratio PS/AR [a]
	Mean (SD) (*wt*%)	CV (%)	Mean (SD) (*wt*%)	CV (%)	
P-CB	1.71 (0.09)	5.3	2.11 (0.09)	4.3	1.23
PA-carbon	4.25 (0.19)	4.5	7.55 (0.39)	5.2	1.78
P–CN-mix	1.93 (0.15)	7.8	13.9 (1.2)	8.4	7.20
P–CN-post	4.46 (0.23)	5.2	8.57 (0.26)	3.0	1.92

[a] Ratio of the P weight content obtained with the piranha solution protocol over the one obtained with the *aqua regia* protocol.

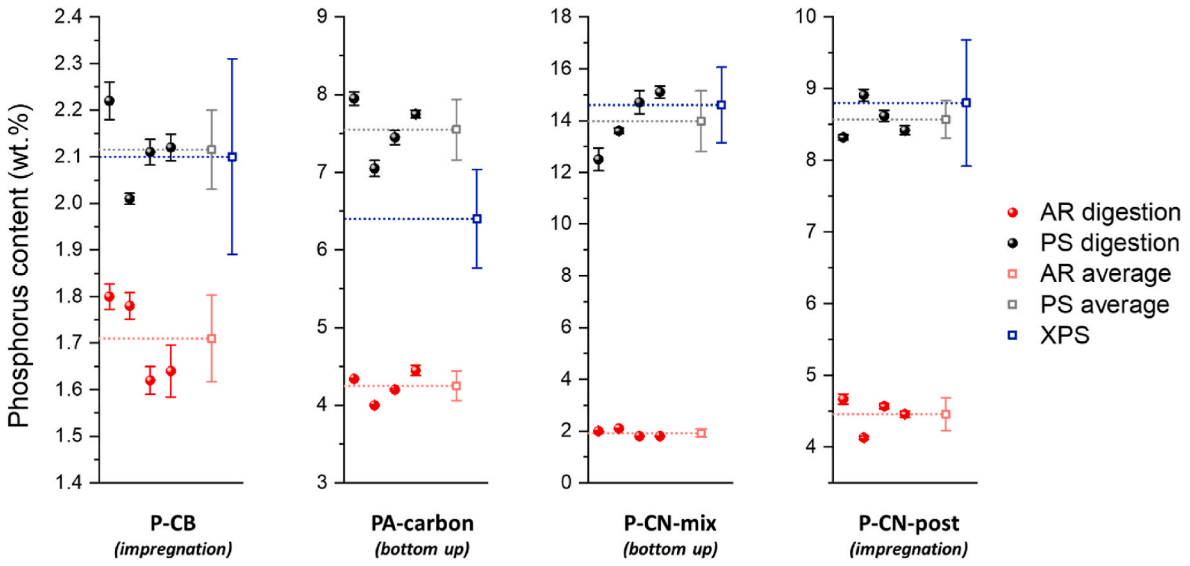

Fig. 3. Comparison of the digestion protocol by *aqua regia* (AR, red) and *piranha solution* (PS, black) for determination of phosphorus content in materials **1**–**4**. Black and red points represent independent digestions of the materials, with the associated error bar of the ICP measurement. Averages on the four samples and associated standard deviations are indicated in faded colors. P contents estimated from XPS are given in blue. (A colour version of this figure can be viewed online.)

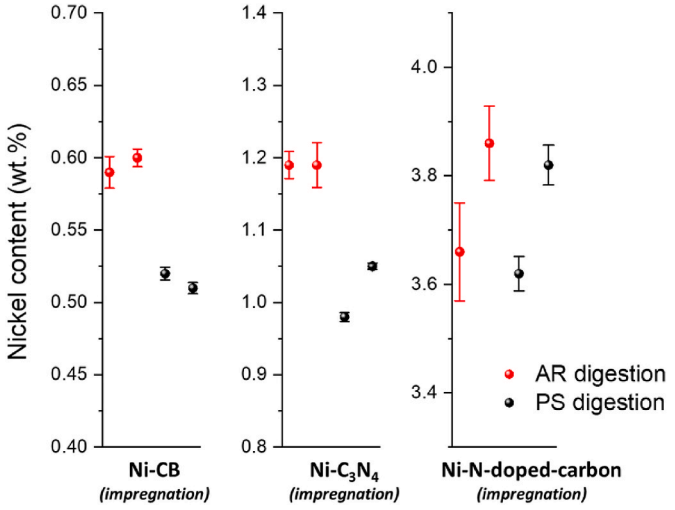

Fig. 4. Comparison of the digestion protocol by *aqua regia* (AR) and *piranha solution* (PS) for determination of nickel content in materials **5**–**7**. Black and red points represent independent digestions of the materials, with the associated error bar of the ICP measurement. (A colour version of this figure can be viewed online.)

(CV_{ICP}) was of 1.2 %, sensibly lower (Table 2). The main source of non-reproducibility therefore originates from the digestion step itself. The determined phosphorus content is, however, systematically much higher with PS than with AR digestion, with ratios PS/AR of 1.23, 1.78, 7.20 and 1.92 for materials **1** to **4**, respectively (Table 2). If any bias is present, it is likely an underestimation due to an over-evaluation of the weighed mass (residual water) or an incomplete digestion. As the decomposition of **2**–**4** is almost total with PS, all the phosphorus atoms are expected to be in solution, leading to correct ICP results. The underestimation with AR protocol, despite a high reproducibility, is therefore due either to P atoms embedded in an undigested part of the material, or to chemical groups that PS could strip and not AR. SEM-EDX measurements performed on the remains of sample **3** after AR digestion confirmed the presence of large amount of leftover phosphorus atoms (Fig. S1). Overall, the error in quantification of heteroatom-content in carbonaceous materials depending on the standard digestion protocol may be massive, up to 620 % here.

On the whole series of P-containing samples, the PS results are in good agreement with estimations derived from XPS measurements (Fig. 3, in blue). Considering an accuracy for XPS of *ca.* 10 %, in line with the report of Shard et al. [12], the differences between ICP and XPS fall within the respective error bars. Worth noting XPS is sensitive to the extreme surface of the material (<5 nm) and to possible contaminations. If the material composition is heterogeneous, for instance due to the localization of the phosphorus atoms at the surface or to a chemical reactivity of exposed groups due to air, the ratios derived from XPS spectra will differ from the average bulk composition. We therefore recommend to propose an element composition on the basis of at least two methods. Here, the congruent findings obtained through ICP and XPS analysis suggest, on one hand, the efficiency and consistency of piranha solution digestion, and, on the other hand, the similarity in chemical composition between the material's surface and its "bulk". Such an agreement is not always guaranteed. For instance, Cheng et al. reported B content values *via* XPS that were three times higher than those determined by ICP [13]. While such discrepancies may not always be reconciled, it is essential to acknowledge and address them in the analysis, and the authors should transparently specify which values they adopt for subsequent analyses.

The results show clear difference depending on the synthesis strategy: impregnation *vs.* bottom-up. In the case of materials **1** and **2** from a post-impregnation and a bottom-up synthesis, respectively, the two digestion protocols have a divergence of 23 % and 78 %. Similarly, for P-doped carbon nitrides, a divergence of 92 % and 620 % are recorded for **3** and **4**, respectively. For comparable materials (**1**–**2** and **3**–**4**), the divergence is higher for samples synthesized *via* a bottom-up approach, and is maximal in the case of material **3** which presents a low porosity (S_{BET} = 4 m^2 g^{-1}) and is totally digested by PS but not by AR (Fig. 1).

If the sample is chemically resistant, *i.e.*, the digestion does not lead to the total dissolution of the matrix (like in the case of well-graphitized carbons), the phosphorus atoms at the core of the material cannot be stripped. On the contrary, post-synthesis impregnation of porous samples essentially leads to doping or functionalization of the surface of the material. The chemical groups targeted for stripping are therefore accessible by the oxidizing solution, and accurate measurements are possible. Chemically resistant carbons with low porosity, synthesized *via* a bottom-up approach are therefore likely to lead to erroneous results, even if the PS protocol is applied. In order to verify that, such non-

porous resistant carbon sample containing P was synthesized from glucose and triphenylphosphine (PPh_3) (see synthesis in SI). According to the discussed findings, the phosphorus content of this sample was clearly different according to ICP (0.14 *wt*%) and SEM-EDX (7.9 *wt*%).

Woo et al. also reported this problem of "inaccessible regions" of the sample, and for instance noted with Transmission Electron Microscopy (TEM) the presence of metal residues still embedded in the carbon layers "*even after iterative acid treatment with aqua regia*" (the catalyst for the bottom-up synthesis comported metals) [33]. Nonetheless, they comment on the differences between the surface composition of the material, as determined from XPS data, and its "bulk" composition, as determined from ICP data. If the carbon matrix is not totally digested, we believe that such discussion is rather delicate as there is uncertainty as to how deep the sample was etched.

3.3. Covalent bonding vs. metal bonding

Heteroatoms such as P or B are directly integrated into the carbon material *via* covalent bonds, and the strength and stability of the corresponding groups vary depending on the speciation. Consequently, certain species may be removed by PS but not by AR. In contrast, metals, alloys, and metal oxides are deposited/coordinated to the carbon matrix and typically held together by metallic-like or ionic bonds of uniform strengths. Then, the digestion solution can either completely decompose all metal containing particles, yielding accurate results, or fail to do so, leading to erroneous results that can be readily identified. The *piranha solution* is specifically used to etch organic compounds leftovers, for instance in microfabrication, whereas the use of *aqua regia* for metal content analysis is usually driven by the capacity of chloride anions to complex the stripped metal cations, such as $[AuCl_4]^-$ for the archetypal example, a specificity irrelevant for the digestion of the organic part. To verify whether the use of PS, required for digesting the "carbonaceous part", may affect the detection of the "metallic part", a parallel set of experiments was conducted on several Ni-containing samples. Nickel was chosen as an archetypal example of supported transition metal, often encountered for catalytic applications. The carbon/carbon nitride-supported nickel materials were obtained by impregnation with an $NiCl_2$ ethanolic solution of carbon black (**5**), carbon nitride (**6**) and N-doped carbon (**7**). They displayed no sharp peaks in XRD corresponding to metallic Ni nor nickel oxide NiO, suggesting that nickel is present as small objects supported on the carbon/carbon nitride (single atoms, clusters, nanoparticles) (**Fig. S2**). Physisorption analysis confirmed the porosity of the carbonaceous materials ($S_{BET} > 550\ m^2\ g^{-1}$), but the carbon nitride is almost non-porous ($S_{BET} = 7\ m^2\ g^{-1}$) (**Fig. S3**). The content of Ni was then quantified after AR or PS digestion. The samples present a limited divergence (PS/AR ratios of respectively 0.87, 0.85 and 0.99 for **5**–**7**), demonstrating no significantly reduced digestion efficiency as to metal analysis (Fig. 4).

3.4. Oxidation chemistry

The exact chemistries at stake in *aqua regia* and *piranha solution* are not always fully understood, mainly because of the high reactivity of these systems and their complex equilibria. However, mixing concentrated nitric and hydrochloric acids produces nitrosyl chloride NOCl and chlorine Cl_2 (Eq (1)), which further react to form nitric oxide NO (Eq (2)), which in turn forms nitrogen dioxide NO_2 (Eq (3)) [34]. The so formed species have high standard reduction potentials E°, between +1.4 V and +1.59 V, attesting to their strong oxidizing power (Table 3). In the case of piranha solution, in concentrated solutions, sulfuric acid H_2SO_4 reacts with hydrogen peroxide H_2O_2 to form the so-called Caro's acid H_2SO_5, or peroxymonosulfuric acid (PMS) (Eq. (4)), displaying an even higher potential of +1.81 V [35]. Some authors also report that PMS decomposition produces oxygen radicals [19].

$$HNO_3 + 3\ HCl \rightarrow NOCl + Cl_2 + 2H_2O \quad (1)$$

$$NOCl \rightarrow NO + 0.5\ Cl_2 \quad (2)$$

$$NO + 0.5\ O_2 \rightarrow NO_2 \quad (3)$$

$$H_2SO_4 + H_2O_2 \rightarrow H_2SO_5 + H_2O \quad (4)$$

The reactivity of PMS in digestion of carbonaceous materials increases in the order carbon black < N-doped carbon < carbon nitrides as indicated in Fig. 1 and discussed forehead. At first, it appears as being in contradiction with the reported stability windows of these last materials toward oxidation, and with the concept of noble carbons [37]. Non doped carbons indeed present a lower standard potential ($E°(C/CO_2) = +0.21$ V) than their N-doped counterparts and carbon nitrides, which displays HOMO states between +1.6 and + 2.1 V. Based on purely thermodynamic arguments, carbons should therefore be more prone to oxidation, and digestion, than C_3N_4, as incidentally demonstrated with open flame experiments [37]. We suggest that the presence of heteroatoms generates more defects on the edges which constitute attack points for PMS. Such an attack can then lead to an "unwinding" of the material, rendering possible the digestion, in opposition to pure carbons only displaying extended aromatic panels difficult to decompose. In the range of conditions accessible for open-vessel digestion (atmospheric pressure, T < 150 °C), carbon black is usually only hydroxylated/oxidized on surface by H_2O_2 or concentrated mineral acids, but not dissolved [38]. Its decomposition therefore remains challenging due to kinetic restrictions.

The standard reduction potentials of active species with AR and PS digestion protocols, as well as other common oxidants are reported in Table 3. The peroxydisulfate $S_2O_8^{2-}$ appears in the electrochemical scale at an even higher potential than HSO_5^- (+2.01 V *vs.* +1.81 V) and should digest the different materials as well. To further verify that, commercial C_3N_4 was mixed with 3 mL of H_2SO_4 95 % and 0.5 g of $K_2S_2O_8$ and

Table 3
Electrochemical properties of most common strong oxidant available in aqueous solutions and/or present in *aqua regia* and *piranha solution*. These data are purely related to thermodynamics and even favorable reactions may not occur for kinetic reasons. All data, except HSO_5^-, were extracted from Ref. [36].

Half-reaction equation		Standard reduction potential E° (V *vs.* NHE)
$O_{3\ (g)} + 2H^+ + 2\ e^-$	$\rightarrow O_{2\ (g)} + H_2O$	2.07
$S_2O_{8(aq)}^{2-} + 2\ e^-$	$\rightarrow 2\ SO_{4(aq)}^{2-}$	2.01
$HSO_{5(aq)}^- + H^+ + 2\ e^-$	$\rightarrow SO_{4(aq)}^{2-} + H_2O$	1.81
$H_2O_2 + 2H^+ + 2\ e^-$	$\rightarrow 2H_2O$	1.76
$Au^+ + e^-$	$\rightarrow Au_{(s)}$	1.69
$2\ NO_{(g)} + 2H^+ + 2\ e^-$	$\rightarrow N_2O_{(g)} + H_2O$	1.59
$NO^+ + e^-$	$\rightarrow NO_{(g)}$	1.46[a]
$Cl_{2\ (aq)} + 2\ e^-$	$\rightarrow 2\ Cl_{(aq)}^-$	1.40
$½\ O_{2\ (g)} + 2H^+ + 2\ e^-$	$\rightarrow H_2O$	1.23

[a] No data could be found for E° of nitrosyl chloride NOCl, but the N–Cl bond is described as loose, its reactivity was therefore estimated as close to that of NO^+.

Table 4
Principal analytical techniques for element composition determination of carbon-based nanomaterials, for phosphorus if unspecified.

Analysis	Range[a]	Advantages/limitations
Materials digestion		
(F)AAS	>50 ppm	- Better sensitivity for B (>1 ppm) - Risk of interferences
GFAAS/ETAAS	>0.5 ppm	- Small quantities required - Possible direct solid analysis - Risk of interferences
ICP-OES/AES	>0.1 ppm	- Straightforward analysis of B, P, more delicate for S (environmental contamination) - Risk of interferences
ICP-MS	>0.05 ppm	- Good sensitivity - Higher cost than ICP-OES
Colorimetry	>0.3 ppm	- Easy to implement - Risk of interferences
Electrons/photons interactions[b]		
SEM-EDX, TEM-EDX	>0.5 wt%	- Analysis depth 1 μm - Sensitive to surface roughness - No reliable detection of B, low accuracy for C, N, O - Possible EDX mapping
XPS	>0.2 wt%	- Analysis depth 2–5 nm - Sensitive to surface roughness - Fine structure analysis - Possible XPS mapping
XRF	>0.1 wt%	- Analysis depth 1 μm - 1 mm - Relative quantification - Difficult analysis for B, C, N and O - Large amount of materials required - Possible mapping for μ-XRF
Neutron activation		
PGNAA	>0.1 wt%	- Not easily accessible - Detection of B, C, N, Si, P, S - Global analysis
Nuclear magnetic resonance		
ss-NMR	>1 wt%	- Low sensitivity - Fine structure analysis - Global analysis

[a] Typical Limit of Quantification (LOQ), expressed in *wt.*% for direct solid analysis and ppm (or mg/L) for liquid analysis after digestion. The LOQ corresponds to 5 times the Limit of Detection (LOD). The values are given as orders of magnitude for standard equipment but are largely dependent on the sample type and composition, the setup, the time of measurement if relevant *etc.* [15,27,40,42,43].
[b] XAS and EELS are also quantitative but not used as primary tool for element composition determination.

heated for 1 h at 90 °C. The cloudy suspension became clear without intense effervescence nor runaway reaction (**Fig. S4**). This apparent comparable efficiency with *piranha solution* first confirms the validity of our analysis. Besides, the use of peroxydisulfate appears as an interesting substitute: the use of PS, particularly at 90 °C, is indeed prohibited in a number of institutions due to its danger [28]. On the contrary, potassium peroxydisulfate salt ($K_2S_2O_8$) and Oxone® salt ($2KHSO_5 \bullet KHSO_4 \bullet K_2SO_4$) are readily available and safer. Such considerations echo those of the field of Advanced Oxidation Processes (AOP) dealing with the degradation of organic compounds in water *via* the use of hydroxyl radicals ($HO^{\bullet}$) or sulfate radicals ($SO_4^{\bullet -}$), liberated by H_2O_2 and persulfates, respectively [39].

3.5. Inter-technique comparison

As aforementioned, diverse analytical methods are employed to ascertain the elemental composition of nanomaterials, each characterized by distinct sensitivities, precision, and robustness (Table 4). A first set of techniques requires the digestion, or mineralization, of the materials in aqueous solutions. Subsequently, the concentration in the target element (*e.g.* B, P, Se) is determined, *via* a calibration curve, relying on:

- Atomic Absorption Spectroscopy (AAS), performed in a continuous mode by atomization in a flame (FAAS) or from a small aliquot atomized at high temperature in a graphite furnace (GFAAS or ETASS).
- Optical Emission Spectroscopy (OES or AES) after ionization in a plasma torch (ICP).
- Mass Spectrometry after ionization by ICP.
- visible spectrophotometry upon formation of a specific colored complex, such as molybdenum blue for P, and curcumin or azomethine for B.

With the exception of FAAS, the sensitivity toward B and P detection is sufficient for the quantification upon digestion of a small fraction of material (<20 mg). These methods offer good precision and accuracy, typically below 5 % [27,40]. Interferences in AAS and OES are mostly due to the presence of metal atoms with absorption/emission bands that overlap with those used for B or P. Note that sulfur analysis is possible *via* ICP-OES and ICP-MS but less straightforward due to its high ionization potential, high blank levels (environmental contamination) and interferences in MS [41]. Besides, its analysis is not compatible with a digestion solution containing sulfuric acid such as piranha solution. As discussed throughout this article, the primary source of error for this set of techniques stems from the decomposition step itself, potentially leading to significant underestimations of concentrations due to incomplete solubilization. Interestingly, recent works report the use of electrothermal vaporization (ETV) for a direct analysis of solid samples when coupled with ICP-OES or GFAAS [27,42].

A second category of techniques is non-destructive and relies on electron-matter interactions (EDX) and photon-matter interactions (XPS, XRF). SEM-EDX and TEM-EDX analysis rely on the detection of X–rays generated upon electron bombardment of the sample. All

elements with Z > 6 (C) are detected if their content exceeds approximately 0.1 *wt%*, while boron detection is feasible but less reliable in presence of carbon [10]. The signal intensity is directly proportional to the concentration of the element, enabling a quantitative approach through calibration curves. However, this approach assumes that the element content is the sole factor influencing signal intensity, and not surface morphology for instance. In practice, achieving high accuracy (relative error below 5%) is possible only with polished samples and the use of certified standards of similar nature. Such ideal conditions are challenging to meet for nanostructured carbonaceous samples, making EDX a semi-quantitative technique. Consequently, it can provide only broad trends and orders of magnitude. In many laboratories, calibration is typically integrated directly into the software used and referred to as "standardless analysis". The analysis parameters are then automatically adjusted to yield a total content of 100%. Accuracy is therefore reliant on the estimation of major elements, such as C or O, whose signals are significantly affected by sample roughness and surface orientation. Based on our experience with carbon nanomaterials, the content of minor elements, such as P or S, can exhibit variations of up to 30% across several spots within a small area. These findings align with the analytical work of Newburie et al., who reported a precision of ±25% [10].

XPS analysis relies on the detection of electrons ejected from the extreme surface of the materials (depth <5 nm) upon excitation with X–rays. Due to its shallow depth of analysis, this technique exhibits high sensitivity to the presence of surface heterogeneities and contamination. Furthermore, the extrapolation of results to represent the "bulk" composition of the material assumes that the surface has not undergone reactions with air or moisture, which could locally alter its composition. XPS can access all elements with Z > 3 (Li) and typically achieves detection limits in the range of 0.1–1 *wt*% [44]. As for EDX, XPS measurements may be analyzed using a set of standard similar materials (rarely done for carbon materials studies) or without standards, *i.e.* only relying on the RSF of the different elements present and a summation to 100 %. Under the latter conditions, the expected accuracy is generally no better than 5–10 % [12]. XPS is nonetheless highly precise, capable of detecting small differences of 1 % in element composition among a series of similar samples treated in the same manner [12]. XPS is less influenced by surface roughness compared to SEM-EDX, but the more intricate background evaluation required for quantification introduces the potential for additional errors.

Finally, X–ray Fluorescence (XRF) analysis relies on the X–rays generated by fluorescence upon excitation of the sample by X–rays. The resulting spectra are analyzed in a manner akin to SEM-EDX, though with larger probed volume [45]. In practice, achieving quantitative analysis of elements from B to F is challenging with energy dispersive analysis (ED-XRF). It necessitates the use of wavelength dispersive detection (WD-XRF) coupled with meticulous sample preparation [46]. The analysis with summation up to 100 % being mostly not accessible, the P content is estimated *via* a calibration curve with materials of similar nature (chemical environment, surface quality). While reported accuracies can be as low as 1 %, note that XRF was primarily developed for the analysis of petrochemical products, oxide materials, or cement, and few studies have applied it to carbonaceous compounds. A precision within the 1–5 % range was reported while investigating phosphorus content in plants and polymers [47,48].

In addition, the instrumental neutron activation analysis (NAA), and more particularly prompt gamma NAA (PGNAA) for light elements such as B and P, is usually recognized as a good standard for the quantification of elements for all types of materials, with quantification limits below 0.1 *wt*% and a precision and accuracy possibly as low as 2 % [49,50]. The detection, which is non-destructive, relies on nuclear physics and is unaffected by the chemical environment, hence a better accuracy due to lower biases. Its access is extremely limited and cannot be considered as a routine technique. Solid state ^{31}P Nuclear Magnetic Resonance (ss-NMR) is also encountered for both B and P without need for enrichment. A fine structure analysis is possible to correlate the different chemical shifts to chemical structures. Due to its relatively lower sensitivity and the complexities involved in sample measurement, this technique is rarely employed as the primary quantification tool.

The validation and comparative assessment of analytical methodologies, such as the analysis of trace metals in carbon nanotubes, typically rely on commercially available certified reference samples or standard reference materials (CRMs/SRMs) [18]. Such standardized materials are nonetheless unavailable for heteroatom-doped carbon nanomaterials and the accuracy of protocols for these materials may only be evaluated through the consistency of results obtained from various analytical techniques, as performed here.

4. Conclusion

In conclusion, we strongly urge the carbon community to consider ICP for the determination of the elemental composition of carbonaceous compounds doped with elements which cannot be quantified by combustion analysis, typically P-doped materials which have been receiving more and more attention in recent years. However, the importance of the digestion protocol should not be neglected. We indeed showed that the use of a *piranha solution* instead of *aqua regia* drastically improves the quality of the open vessel digestion, leading to a more accurate determination of the P content and to results in line with XPS measurements. Although the use of *piranha solution* could not overcome the chemical recalcitrance of carbons such as commercial carbon black, we demonstrated that it can achieve the total digestion with a simple open-vessel protocol of several heteroatom-doped carbonaceous materials, including carbon nitrides. In view of the above, one should consider a number of precautions with regard to the digestion step, hence the following recommendations:

- Systematically indicate the digestion protocol (oxidant, acid, proportions, temperature, duration, *etc.*), particularly when no total digestion of the carbon sample is observed.
- For series of new materials of unknown chemistry, first determine which digestion protocol is best for ICP (use of microwave, *aqua regia*, *piranha solution,* muffle furnace, *etc.*).
- Estimate the error bar related to the digestion step with independent digestions and do not only consider that of the ICP measurement itself.
- Good reproducibility of the protocol as to the “digestion step” is not synonymous with high accuracy.
- If possible, check the absence of the element of interest after digestion if the carbon matrix is not destroyed.
- Take into consideration possible biases arising from sample moisture, weighing accuracy (ideally more than 10 mg), possible filtration prior to ICP measurement, and evaporation or precipitation of the targeted element during digestion or subsequent neutralization.

CRediT authorship contribution statement

Rémi F. André: Conceptualization, Investigation, Writing – original draft. **Jessica Brandt:** Investigation. **Johannes Schmidt:** Investigation, Writing – review & editing. **Nieves López-Salas:** Writing – review & editing. **Mateusz Odziomek:** Supervision, Writing – review & editing. **Markus Antonietti:** Funding acquisition, Supervision, Writing – review & editing.

Declaration of competing interest

The authors declare that they have no known competing financial interests or personal relationships that could have appeared to influence the work reported in this paper.

Acknowledgements

The Max Planck Society is gratefully acknowledged for financial support. B. Badamdorj and H. Runge are acknowledged for SEM-EDX measurements. The Deutsche Forschungsgemeinschaft (DFG) is acknowledged for the "Germany's Excellence Strategy–EXC 2008-390540038–UniSysCat" funding.

Appendix A. Supplementary data

Supplementary data to this article can be found online at https://doi.org/10.1016/j.carbon.2024.118946.

References

[1] J.P. Paraknowitsch, A. Thomas, Doping carbons beyond nitrogen: an overview of advanced heteroatom doped carbons with boron, sulphur and phosphorus for energy applications, Energy Environ. Sci. 6 (10) (2013).
[2] W. Kiciński, M. Szala, M. Bystrzejewski, Sulfur-doped porous carbons: synthesis and applications, Carbon 68 (2014) 1–32.
[3] C.N.R. Rao, K. Gopalakrishnan, A. Govindaraj, Synthesis, properties and applications of graphene doped with boron, nitrogen and other elements, Nano Today 9 (3) (2014) 324–343.
[4] A.M. Puziy, et al., Phosphorus-containing carbons: preparation, properties and utilization, Carbon 157 (2020) 796–846.
[5] G. Hasegawa, et al., High-level doping of nitrogen, phosphorus, and sulfur into activated carbon monoliths and their electrochemical capacitances, Chem. Mater. 27 (13) (2015) 4703–4712.
[6] H. Tan, et al., Phosphorus- and nitrogen-doped carbon nanosheets constructed with monolayered mesoporous architectures, Chem. Mater. 32 (10) (2020) 4248–4256.
[7] M.A. Patel, et al., P-doped porous carbon as metal free catalysts for selective aerobic oxidation with an unexpected mechanism, ACS Nano 10 (2) (2016) 2305–2315.
[8] J. Zhang, et al., A metal-free bifunctional electrocatalyst for oxygen reduction and oxygen evolution reactions, Nat. Nanotechnol. 10 (5) (2015) 444–452.
[9] Y. Zhang, et al., Phosphorus-doped carbon nitride solid: enhanced electrical conductivity and photocurrent generation, J. Am. Chem. Soc. 132 (18) (2010) 6294–6295.
[10] D.E. Newbury, N.W. Ritchie, Is scanning electron microscopy/energy dispersive X-ray spectrometry (SEM/EDS) quantitative? Scanning 35 (3) (2013) 141–168.
[11] T. Susi, T. Pichler, P. Ayala, X-ray photoelectron spectroscopy of graphitic carbon nanomaterials doped with heteroatoms, Beilstein J. Nanotechnol. 6 (2015) 177–192.
[12] A.G. Shard, Practical guides for x-ray photoelectron spectroscopy: quantitative XPS, J. Vac. Sci. Technol. A 38 (4) (2020).
[13] D.-W. Wang, et al., Synthesis and electrochemical property of boron-doped mesoporous carbon in supercapacitor, Chem. Mater. 20 (22) (2008) 7195–7200.
[14] S. Chu, et al., Selenium-doped carbon: an unexpected efficient solid acid catalyst for Beckmann rearrangement of ethyl 2-(2-aminothiazole-4-yl)-2-hydroxyiminoacetate, Catal. Commun. 129 (2019).
[15] C.R. Brundle, C.A.J. Evans, S. Wilson, *Encyclopedia Of Materials Characterization*. Materials Characterization Series, Elsevier, 1992.
[16] Chemistry Resources for Lab Techs and Spectroscopists, Inorganic Adventures, September 28, 2023, https://www.inorganicventures.com/education.
[17] H. Matusiewicz, Sample preparation for inorganic trace element analysis, Phys. Sci. Rev. 2 (5) (2017).
[18] F.R. Simoes, et al., Elemental quantification and residues characterization of wet digested certified and commercial carbon materials, Anal. Chem. 88 (23) (2016) 11783–11790.
[19] P.D. Wathudura, et al., Microwave and open vessel digestion methods for biochar, Chemosphere 239 (2020) 124788.
[20] K.X. Yang, et al., Evaluation of sample pretreatment methods for multiwalled and single-walled carbon nanotubes for the determination of metal impurities by ICPMS, ICPOES, and instrument neutron activation analysis, J. Anal. Atomic Spectrom. 25 (8) (2010).
[21] S.R. Krzyzaniak, et al., Determination of inorganic contaminants in carbon nanotubes by plasma-based techniques: overcoming the limitations of sample preparation, Talanta 192 (2019) 255–262.
[22] J.-H. Lim, V.G. Bairi, A. Fong, Quantification of impurities in carbon nanotubes: development of ICP-MS sample preparation methods, Mater. Chem. Phys. 198 (2017) 324–330.
[23] S.P. Patole, et al., An evaluation of microwave-assisted fusion and microwave-assisted acid digestion methods for determining elemental impurities in carbon nanostructures using inductively coupled plasma optical emission spectrometry, Talanta 148 (2016) 94–100.
[24] S.M. Cruz, et al., Microwave-induced combustion method for the determination of trace and ultratrace element impurities in graphite samples by ICP-OES and ICP-MS, Microchem. J. 123 (2015) 28–32.
[25] F.R.F. Simoes, et al., Validation of alkaline oxidation as a pre-treatment method for elemental quantification in single-walled carbon nanotubes, Anal. Methods 11 (14) (2019) 1884–1890.
[26] S.R. Mortari, et al., Fast digestion procedure for determination of catalyst residues in La- and Ni-based carbon nanotubes, Anal. Chem. 82 (10) (2010) 4298–4303.
[27] W. Kiciński, S. Dyjak, Transition metal impurities in carbon-based materials: pitfalls, artifacts and deleterious effects, Carbon 168 (2020) 748–845.
[28] H.G. Schmidt, Safe piranhas: a review of methods and protocols, ACS Chem. Health Saf. 29 (1) (2021) 54–61.
[29] T.R. Gengenbach, et al., Practical guides for x-ray photoelectron spectroscopy (XPS): interpreting the carbon 1s spectrum, J. Vac. Sci. Technol. A 39 (1) (2021).
[30] A.M. Puziy, et al., XPS and NMR studies of phosphoric acid activated carbons, Carbon 46 (15) (2008) 2113–2123.
[31] M. Ayiania, et al., Deconvoluting the XPS spectra for nitrogen-doped chars: an analysis from first principles, Carbon 162 (2020) 528–544.
[32] Y. Wang, et al., Evolution of phosphorus-containing groups on activated carbons during heat treatment, Langmuir 33 (12) (2017) 3112–3122.
[33] C.H. Choi, S.H. Park, S.I. Woo, Phosphorus–nitrogen dual doped carbon as an effective catalyst for oxygen reduction reaction in acidic media: effects of the amount of P-doping on the physical and electrochemical properties of carbon, J. Mater. Chem. 22 (24) (2012).
[34] L.J. Beckham, W.A. Fessler, M.A. Kise, Nitrosyl chloride, Chem. Rev. 48 (3) (1951) 319–396.
[35] M. Spiro, The standard potential of the peroxosulphate/sulphate couple, Electrochim. Acta 24 (3) (1979) 313–314.
[36] S.G. Bratsch, Standard electrode potentials and temperature coefficients in water at 298.15 K, J. Phys. Chem. Ref. Data 18 (1) (1989) 1–21.
[37] M. Antonietti, M. Oschatz, The concept of "noble, heteroatom-doped carbons," their directed synthesis by electronic band control of carbonization, and applications in catalysis and energy materials, Adv. Mater. 30 (21) (2018) e1706836.
[38] J. Zhu, et al., Engineering surface groups of commercially activated carbon for benzene hydroxylation to phenol with dioxygen, Ind. Eng. Chem. Res. 58 (44) (2019) 20226–20235.
[39] J. Lee, U. von Gunten, J.H. Kim, Persulfate-based advanced oxidation: critical assessment of opportunities and roadblocks, Environ. Sci. Technol. 54 (6) (2020) 3064–3081.
[40] M.A. Bechlin, J.A. Gomes Neto, J.A. Nóbrega, Evaluation of lines of boron, phosphorus and sulfur by high-resolution continuum source flame atomic absorption spectrometry for plant analysis, Microchem. J. 109 (2013) 134–138.
[41] J. Giner Martínez-Sierra, et al., Sulfur analysis by inductively coupled plasma-mass spectrometry: a review, Spectrochim. Acta B Atom Spectrosc. 108 (2015) 35–52.
[42] D. Wieczorek, et al., Determination of phosphorus compounds in plant tissues: from colourimetry to advanced instrumental analytical chemistry, Plant Methods 18 (1) (2022) 22.
[43] S. Kanno, et al., Performance and limitations of phosphate quantification: guidelines for plant biologists, Plant Cell Physiol. 57 (4) (2016) 690–706.
[44] A.G. Shard, Detection limits in XPS for more than 6000 binary systems using Al and Mg Kα X-rays, Surf. Interface Anal. 46 (3) (2014) 175–185.
[45] M. Mantler, et al., Quantitative analysis, in: Handbook of Practical X-Ray Fluorescence Analysis, 2006, pp. 309–410.
[46] P.M. Farkov, L.N. Il'icheva, A.L. Finkel'shtein, X-Ray fluorescence determination of carbon, nitrogen, and oxygen in fish and plant samples, J. Anal. Chem. 60 (5) (2005) 426–430.
[47] M.R. Fuh, W.E. Rochefort, Analysis of residual phosphorus in poly(p-phenylene benzoxazole), PBO, film by x-ray fluorescence (XRF) spectrometry, Talanta 41 (12) (1994) 2087–2090.
[48] S. Reidinger, M.H. Ramsey, S.E. Hartley, Rapid and accurate analyses of silicon and phosphorus in plants using a portable X-ray fluorescence spectrometer, New Phytol. 195 (3) (2012) 699–706.
[49] L. Zhao, et al., Determination of carbon, nitrogen, and phosphorus in cattail using thermal neutron prompt gamma activation analysis, J. Radioanal. Nucl. Chem. 277 (1) (2008) 275–280.
[50] C.L. Schutz, et al., Intercomparison of inductively coupled plasma mass spectrometry, quantitative neutron capture radiography, and prompt gamma activation analysis for the determination of boron in biological samples, Anal. Bioanal. Chem. 404 (6–7) (2012) 1887–1895.